



# Primary evaluation of the use and refining of Al scrap recovered from a landfill in Belgium

M.Sc. Hugo Lucas<sup>1</sup>, M.Sc. Cong Li<sup>1</sup>, M.Sc. Cristina García López<sup>2</sup>,  
M.Sc. Juan Carlos Hernández Parrodi<sup>4</sup>, M.Sc. Devrim Gürsel<sup>3</sup>, Prof. Dr.-Ing. Bernd Friedrich<sup>1</sup>,  
Prof. Dr.-Ing. Thomas Pretz<sup>2</sup>, Prof. Dr.-Ing. Hermann Wotruba<sup>3</sup>

RWTH Aachen University

<sup>1</sup> IME Process Metallurgy and Metal Recycling,  
Intzestraße 3

<sup>2</sup> IAR Department of Processing and Recycling  
Wüllnerstraße 2

<sup>3</sup> AMR Unit of Mineral Processing  
Lochner Straße 4 – 20  
Aachen, Germany

<sup>4</sup> Renewi Belgium SA/NV  
Gerard Mercatorstraat 8  
Lommel, Belgium.

---

**Keywords:** Aluminium scrap, non-ferrous metal recovery, enhanced landfill mining, metal sorting technologies, refining

## Abstract

This preliminary evaluation of aluminium recovered from a municipal solid waste landfill was carried out as part of the EU Training Network for Resource Recovery through Enhanced Landfill Mining (NEW-MINE). NEW-MINE is laying the foundations for a resource-efficient and environmentally driven industry that couples enhanced landfill mining (ELFM) with production processes. Among others, ELFM combines remediation strategies and innovative technologies for the recovery of potentially secondary raw materials and the production of high added-value products.

To this day, there is no reliable data about the quality of metals recovered in ELFM. In general, excavated materials are processed mechanically through different steps, such as classifying, shredding and separation. In the case of metal recovery, mechanical processing schemes use magnet separators to extract ferrous metals and eddy-current separators to recover nonferrous metals, such as aluminium, copper, zinc and lead. Within NEW-MINE, a case study was carried out on metals excavated from a Belgian landfill in the municipality of Mont-Saint-Guibert, where nonferrous metals



were extracted using eddy-current separation. The separation of aluminium was made using two different sorting technologies; optical sorting based in infrared spectrum and X-ray sorting. Subsequently, the aluminium was melted in a tilting rotary kiln using a slag of  $\text{KCl-MgCl-CaF}_2$  as oxide collector and atmosphere barrier. Finally, the quality of aluminium was evaluated in terms of polluted metals and oxides, which were influenced by the sorting technology used.

Impurities and oxides in the aluminium scraps showed values of around 50 % and 30 % for the fine and coarse fractions, respectively. The impurities had negative effects on the detection yield of both techniques. However, the X-ray sensor was less affected by the presence of impurities and allowed a better accuracy to maximize Al separation. The purity after refining reached values between 96 % and 99 %. Several of the pollutants found on the aluminium were closely related to the employed separation techniques and the impurities attached to aluminium scrap itself. These alloying elements can be lowered by a previous firing. Final results demonstrated that old aluminium scrap can be successfully recycled despite been buried for decades.

## 1 Introduction

In general, enhanced landfill mining (ELFM) aims at an integrated waste valorisation as waste-to-material and waste-to-energy respecting most astringent social and environmental criteria [1]. In particular, ELFM within the framework of the EU Training Network for Resource Recovery through Enhanced Landfill Mining (NEW-MINE) couples the latter with innovative technologies for the recovery of upcycled and high added-value products, such as metals, syngas, inorganic polymers and construction materials, among others. Ferrous (Fe) and non-ferrous (NFe) metals belong to the recoverable materials with highest market value in ELFM [2]. In most cases, metals remain buried for several decades before site remediation, and during this time they might experience strong corrosion and pollution with organic and inorganic matter. Thus, the study of their quality and extent of recovery is of high interest and critical relevance.

Previous landfill mining studies have shown that landfills could be a source of Fe and NFe metals, as well as of other secondary raw materials, such as plastics, refuse derived fuel, construction aggregates and glass, among others [3, 4]. For instance, aluminium (Al) typically represents around 65 wt.-% of NFe metals from municipal solid waste (MSW) [5], which a few decades ago was sent to landfills together with the rest of the waste with poor or even without recovery of NFe metals.

Al is one of the most ignoble elements of nature. When this metal is in contact with other metal oxides at high temperature, the oxides tend to be reduced which in turn cause a pollution of aluminium. This is reason why refining plants demand high quality scraps to prevent undesired alloying going to the metallic phase.

In the NEW-MINE case study waste was excavated and mechanically pre-processed at a landfill site in Belgium [6, 7]. Samples of the excavated waste after pre-treatment were taken and analysed in order to determine their composition and characteristics, from which the amount of NFe fraction was determined and samples for the laboratory analysis of this study were obtained [6, 7]. The pre-



sent study is focused on the results of the analysis of NFe metallic concentrates extracted from the landfill in question, particularly on the quality and extent of recovery of Al scrap.

## 2 Materials and methods

### 2.1 Site description

The excavated landfill was a disposal site for MSW, construction and demolition waste and non-hazardous industrial waste located in the municipality of Mont-Saint-Guibert (MSG), Belgium (Figure 1) [6 – 8]. This site has a total area of about 44 ha [9] and has been in operation since the late 1960's [10]. The excavation took place at the old landfill area (red delimited area in Figure 1 (left)) [6, 7], which has a varying depth of 30-60 m and stores more than 5.7 million m<sup>3</sup> of waste materials [6 – 11]. This area has an estimated size of 14 ha [6, 7].



Figure 1: MSG landfill (left) and excavation zone (right) [7].

A smaller zone within the old area (white delimited area in Figure 1 (right)) was selected for the excavation of waste with the aid of geophysical exploration [6, 7]. This area had around 130 m<sup>2</sup> and was excavated to a depth of about 5 m (excluding cover layer) [6, 7]. Further information about this landfill site can be found in García López et al., 2019 [6] and Hernández Parrodi et al., 2018 [7].

### 2.2 Excavation works and material pre-processing

A total amount of about 370 ton of landfill waste were excavated (Figure 2a) from the landfill in question in August-September 2017 [6, 7]. The excavated material was processed with a ballistic separator (Figure 2b) in two steps [6, 7]. This machine splits the input material into 3 different outputs: 3-D, 2-D and under-screen fractions [6, 7]. The first ballistic separation step was carried out using a screen of 200 mm, while the second step was done with a screen of 90 mm [6, 7]. In the MSG landfill case study, the coarse fractions correspond to the materials with a particle size > 90 mm (3-D >200 mm, 2-D > 200 mm, 3-D 200 – 90 mm and 2-D 200 – 90), whereas the fine fractions to the fractions < 90 mm [6, 7].

After the ballistic separation, only the 2-D fraction > 200 mm was processed with a mobile shredder equipped with a built-in over-belt magnetic separator (Figure 2c), where Fe metals were recovered



onsite [6, 7]. The NFe metal content of all other fractions was determined via manual characterization at the laboratory.

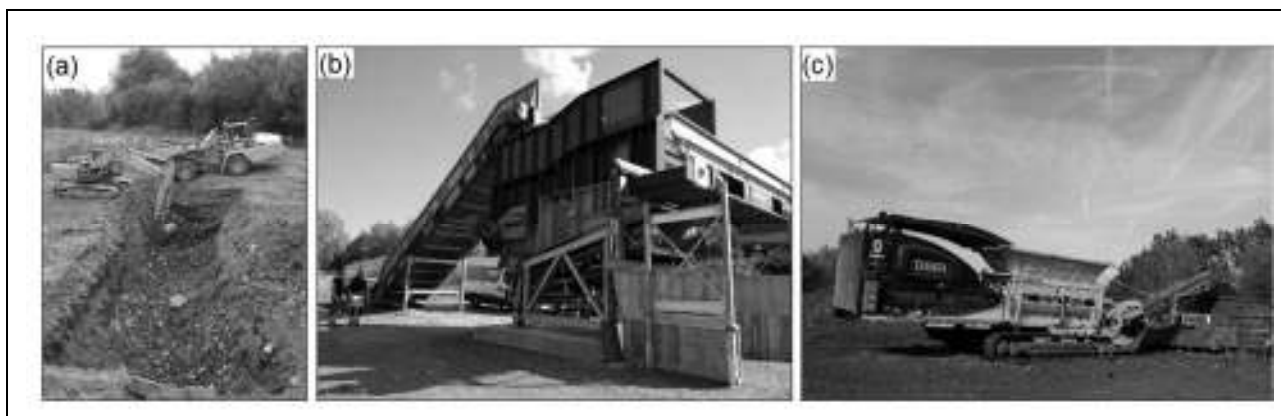


Figure 2: (a) Excavator and dumper; (b) ballistic separator; (c) mobile shredder.

In the NEW-MINE case study around 20 wt.-% of the total excavated material in raw state corresponded to coarse fractions (material  $\geq 90$  mm) and 80 wt.-% to fine fractions (material  $< 90$  mm) [6, 7]. More details about the excavation works can be found in García López et al, 2019 [6] and Hernández Parrodi et al., 2018 [7].

## 2.3 NFe metals content and separation

In order to determine the composition and characteristics of the excavated material, approximately 900 kg of representative samples were taken from all output fractions of the ballistic separation process [6, 7]. These samples were analysed at the Department of Waste Processing and Recycling (IAR, RWTH Aachen University).

According to the particle size of the material flow, different routes to extract metals were chosen: The NFe metals in the coarse fractions ( $> 200$  mm and  $200 - 90$  mm) were selected manually, with the difference that the fraction  $200 - 90$  mm was first dried and sieved. The fine fractions were also dried and sieved prior to Fe metal recovery. After magnetic separation, the fine fractions were divided in three particle size ranges in order to enhance Fe and NFe metals recovery with magnetic and eddy-current-separators. These particle size ranges were  $90 - 30$  mm,  $30 - 10$  mm and  $10 - 4.5$  mm. The fraction  $< 4.5$  mm from the fine fractions was not processed further regarding Fe and NFe metals recovery.

## 2.4 Al sorting

Sorting technologies use different sensors to separate and detect materials. Among the most common technologies X-ray transmission (XRT) and Near-infrared (NIR) detectors can be used to recognise and separate metals.



For this study, the NFe fractions were first analysed with a portable XRF analyser (Thermo Fisher NITON XL3t 600), weighed and marked with a red cross. After this preliminary quantitative analysis, which showed the exact proportion of Al, the samples were randomly bonded in a white piece of paper and then scanned by each method. Pieces identified as Al for each method were sorted again by hand and weighed for quantitative analysis.

### 2.4.1 Separation of Al with X-ray sorting

The used X-ray detector is a luggage scanner based on dual energy X-ray transmission. The X-rays are generated by a 140 kV high-performance generator and can be categorized as hard X-rays. They are commonly used to investigate the inside of an object. The generated image of the detector has a resolution of 481 x 576 with a colour depth of 24-bit. The objects are classified in three different colours depending on the effective atomic weight  $Z_{\text{eff}}$  of the fractions in the object. In the generated image, light elements ( $Z_{\text{eff}} < 10$ ) are orange, medium-heavy elements ( $Z_{\text{eff}}: 10 - 15$ ) are green and heavy elements ( $Z_{\text{eff}}: 15 - 56$ ) are blue. Depending on the elements and thickness of the object, the analysis of the sensor results in an overlay of the colours [10].

Referring to Table 1, green is an indication for Al and blue is an indication for copper and zinc. With this classification, separation of Al from the NFe concentrates has been possible.

Table 1: Colouring according to different materials [12].

Colour gradient	Effective atomic weight	Pure materials and compounds
	< 10	Light elements: hydrogen, carbon, nitrogen, oxygen, and their compounds, organic materials, plastics like acryl, paper, textiles, food products, wood and water, among others.
	10 – 15	Medium-heavy elements: sodium, light metals like magnesium and <b>aluminium</b> and their oxides.
	15 – 56	Heavy elements: titan, chrome, iron, nickel, <b>copper</b> , <b>zinc</b> , tin and silver, among others.

Figure 3 shows an example of a measurement with the XRT sensor with a photo of the material and two processed images of the XRT sensor. Figure 3a shows a sample of NFe metals stuck randomly on a white paper and where the Al pieces were marked with a red cross to compare the detection efficiency of both sensors. The two XRT images (Figure 4a and 4b) present two different processing settings of the sensor. This helps to detect lighter elements (orange-green particles) of the sample. In this example, the blue highlighted copper / zinc particles are clearly to differentiate from the other green and orange mostly Al parts. The next step is to sort the detected particles by hand, weigh them and do a measurement with the same sample with the NIR sensor.

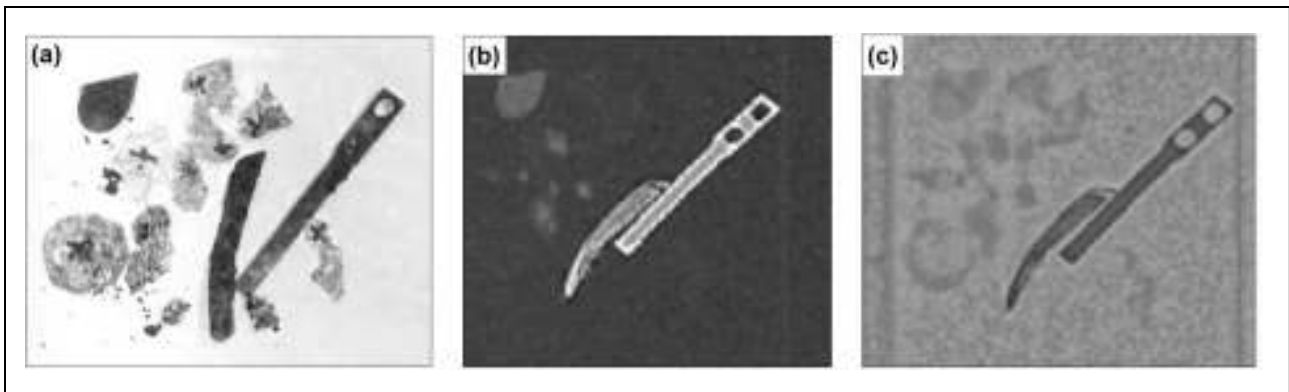


Figure 3: (a) NFe sample; (b) XRT image with high contrast; (c) XRT with low contrast.

### 2.4.2 Separation of Al with near-infrared sorting

For the NIR sensor measurements, a NIR hyperspectral imaging system from EVK DI KERSCHHAGGL GMBH was used. The sensor operates in a spectral range from 1,000 to 1,700 nm. The width of one pixel is 1.08 mm (based on 139 pixel distributed on 150 mm).

After taking images with the NIR-sensor, the raw spectrum of each pixel as a function of wavelength and intensity of the detected radiation is shown. Based on the first derivative and normalization of the spectrum, characteristic areas and peaks in the spectrum have to be analysed. When comparing the different spectra of the objects, a material identification can be done along with an assignment of colours for each spectrum. The result is a coloured-classified image of the samples.



Figure 4: (a) NFe sample; (b) NIR without image processing; (c) NIR with image processing.

Figure 4 shows an example of the measurements with a VIS image, a raw NIR image without any classification (Figure 4b) and the coloured-classified image of the sample (Figure 4c). Particles with Al parts should appear red and the other non-Al parts should appear green. In reality, this is difficult to achieve because of contamination, similar spectra, mixed spectra and other effects. In particular, these samples (Figure 4) differ in the spectra compared to pure aluminium, copper and zinc samples due to corrosion and pollution of the samples surface. Therefore, in this case a characterisation could be done due to different weathering conditions of the metals.





Al sorting is summarised in the flow diagram in Figure 5.

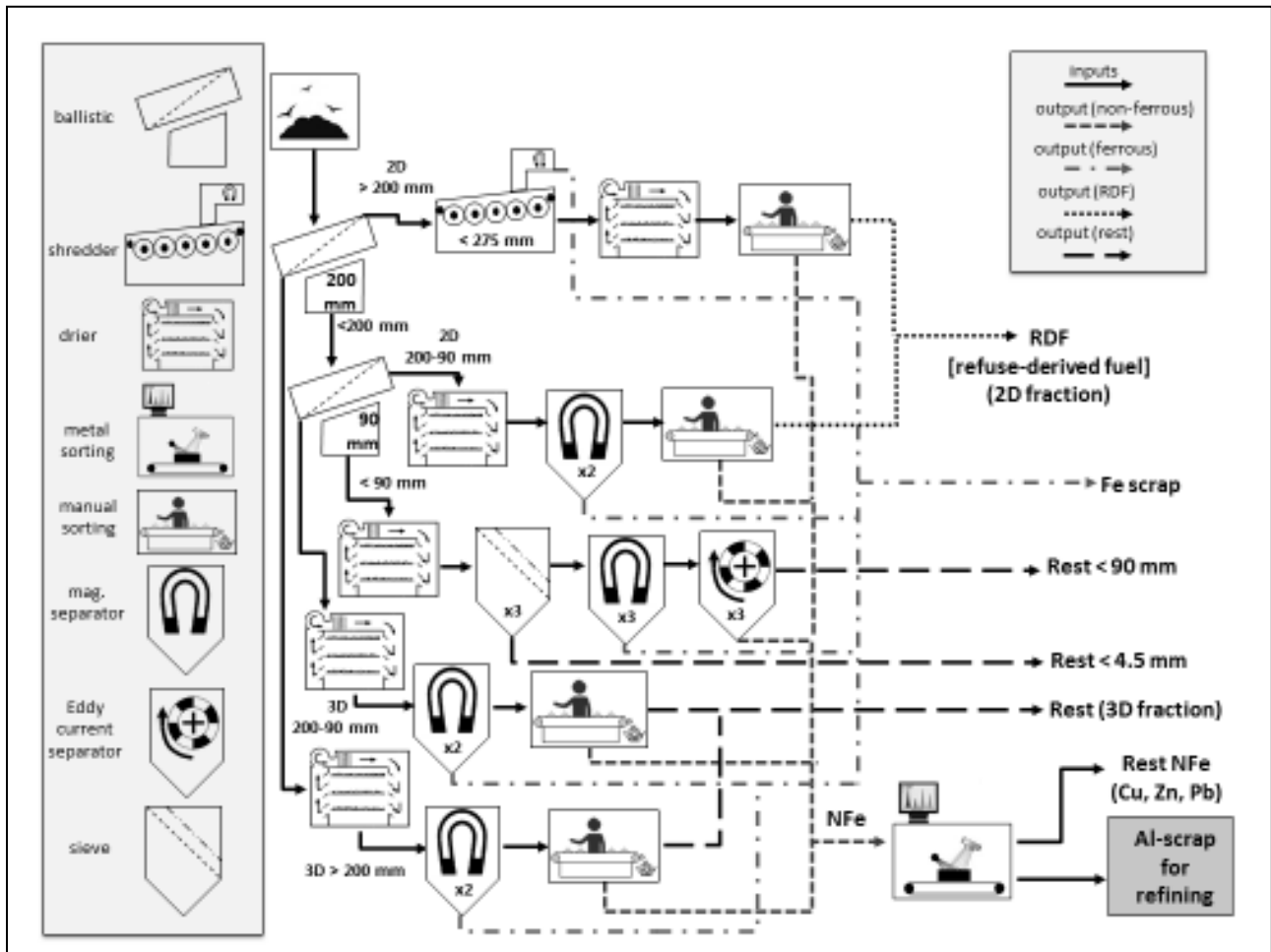


Figure 5: Schema of Al processing from landfill waste.

## 2.5 Salt refining

Al scrap recovered using the XRT sensor were selected for the refining. A mini tilting rotary furnace (TRF) as shown in Figure 6 was used for the smelting of Al scrap. The furnace heated by electrical resistance, use a ceramic crucible with a volume of 0.3 l. This device can be tilted for the vertical position ( $0^\circ$ ) to  $65^\circ$  and the rotation speed can also be adjusted between 0 to 40 ppm.

For all the experiments, a NaCl-25 % KCl salt mix with 5 wt.-% cryolite was used. The temperature set up at  $750^\circ\text{C}$  and the rotation at 30 rpm. Thoraval M. et al. [13] demonstrated that with this rotational speed, a Froude number equivalent to those used by industrial TRF can be obtained [14]. A ratio Al scrap/salt was chosen at 0.33 due to a high content of impurities.

In this work, only the fraction 200 – 90 mm and 90 – 4.5 mm were studied and compared.



Large pieces of Al (> 20 mm) were previously sliced. Around 200 g of scrap was used in each experiment. Six trials were performed, three related to the fraction  $\geq 90$  mm and three for the < 90 mm.

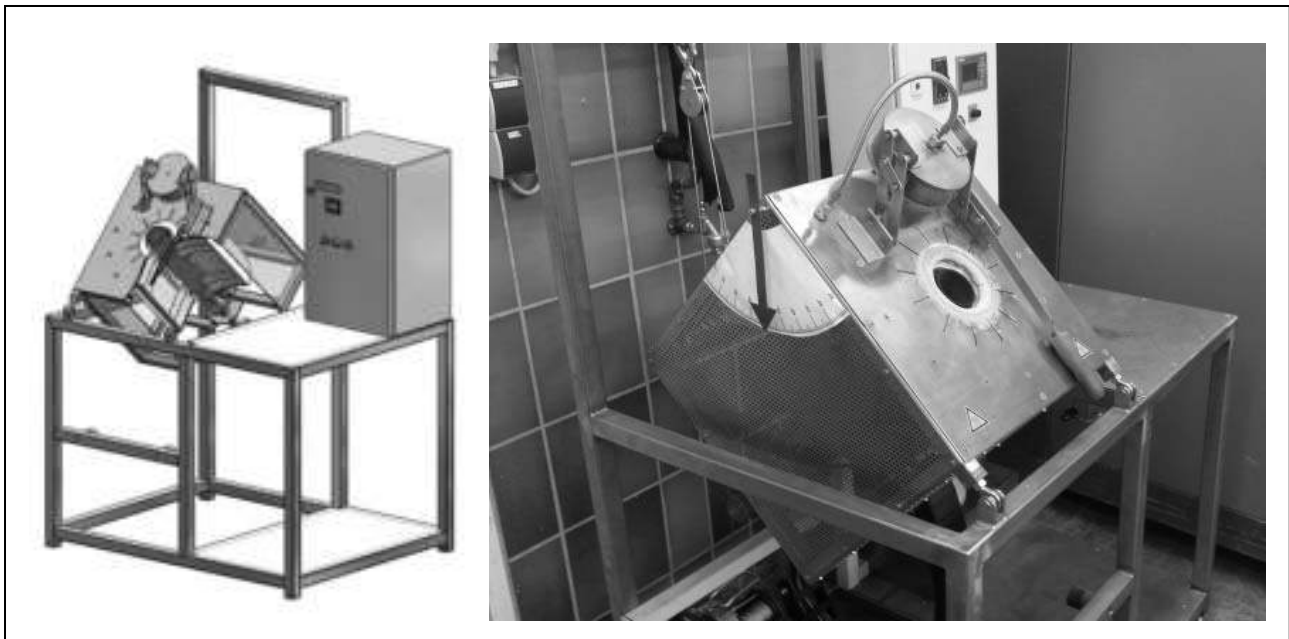


Figure 6: Mini-tilting rotary furnace (TRF) used for Al refining.

### 3 Results

#### 3.1 Excavation and metal separation

As shown in Figure 5, the excavated material was divided into several fractions using a ballistic separator. Related to the interest of this article, three metallic fractions were extracted, pieces > 200 mm, 200 – 90 mm, and finally, the finest fraction comprised among 90 – 4.5 mm. The processing of the fraction below 4.5 mm was considered economically unsuitable for the extraction of metals. Metals (fine and coarse fractions) represented 2.9 wt.-% of the input material wherein NFe metal concentrates are 16.5 % of it.

In general terms, the distribution of metals in landfill waste follows approximately the same distribution than the input material (see Table 2). Since the finest fraction (90 – 4.5 mm), from which metals were extracted, concentrates the 74 % of NFe, as it can be seen on the table above, and the fine fractions (< 90 mm) represent 78 % of the total excavated landfill waste.

Table 2: Material distribution obtained with the ballistic separators.

Screening results [wt.-%]	Input Material	Ferrous (2.43 % input)	Nonferrous (0.48 % input)
> 200 mm	6 %	7 %	8 %
200 – 90 mm	16 %	24 %	18 %
< 90 mm	78 %	69 %	74 %





The Figure 7a shows the results of Al scrap extracted by manual sorting from the NFe concentrates and, subsequently, confirmed using a portable XRF apparatus. Regarding the Al recovered; the results were grouped in three categories: Al packages, Al foils and Al alloys, which contain the scraps that did not fit the previous two categories. It is clear that the contribution of Al foils, such as those we use in our kitchen, and packages, like cans or Tetra-packs<sup>®</sup>, are driving the finest fraction (< 90 mm). In case of coarse fractions ( $\geq 90$  mm), Al came mainly from construction and demolition materials. The origin of this Al can have a strong influence on the type and proportions of pollutants found after the refining.

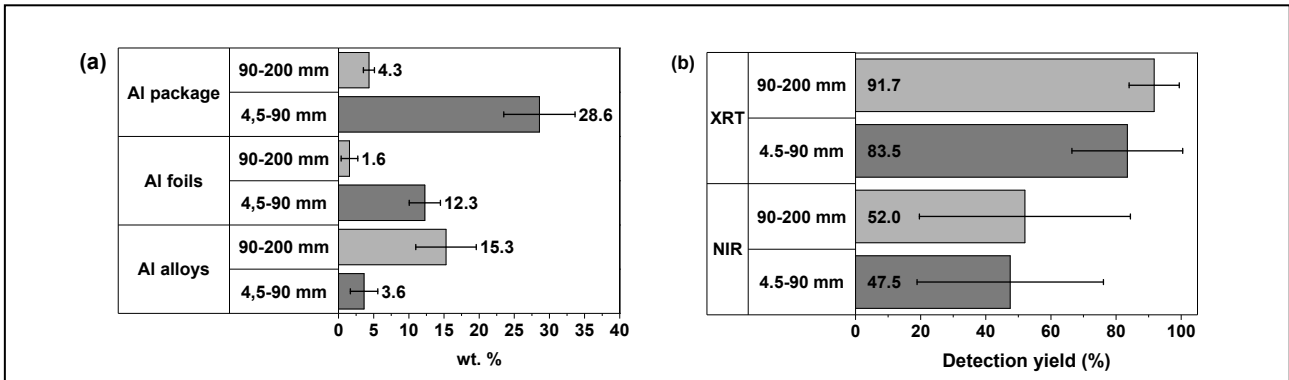


Figure 7: Al sorting: (a) by category, (b) detection yields of NIR and XRT sensors.

## 3.2 Al sorting

### 3.2.1 NIR detectors

The spectra detected by the sensor and used for the colour-classification is shown in Figure 8. As in Figure 9c, the colours red and green stand for Al and non-Al parts. The white curve presents the spectrum of the background which in this case was a white paper. The curve of the Al and non-Al curves showed similar trends when the scraps had strongly polluted. However, a correct classification of the materials is possible when the surface of the metals were clean.

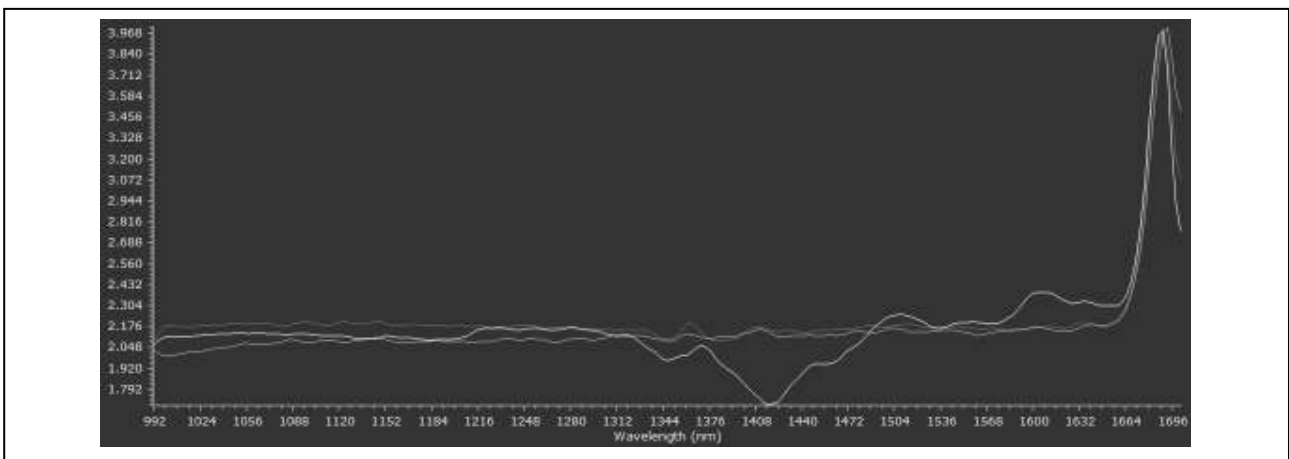


Figure 8: NIR spectra of the materials in the sample.



The reliability on the NIR technology will depend on the degree of contamination of the particle. In case of the analysed samples, the detection yield was around 50 % for both fractions (200 – 90 mm and 90 – 4.5 mm) with an strong standard deviation (see Figure 7b-NIR).

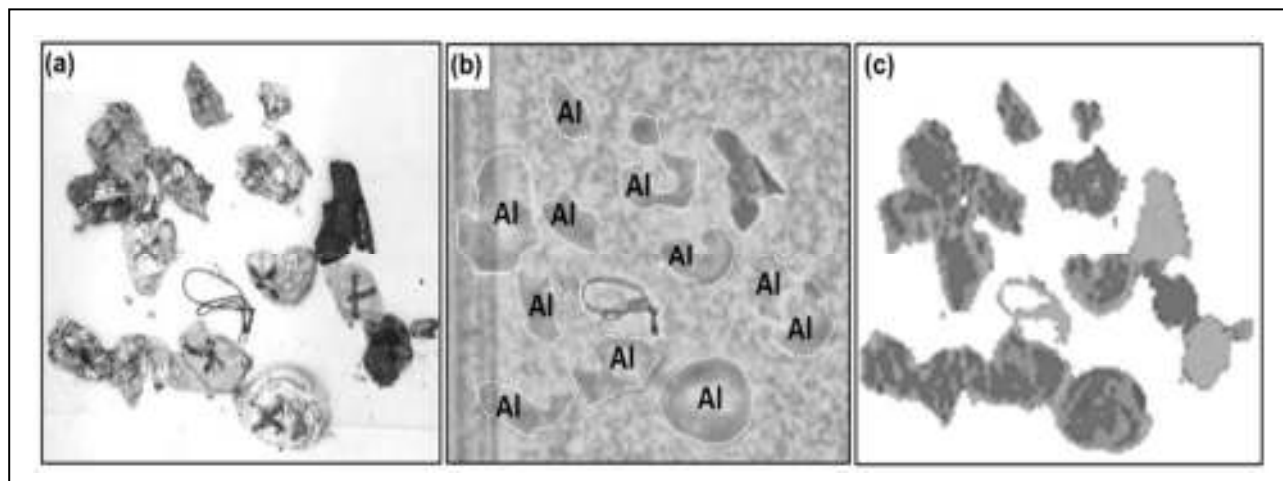


Figure 9: Sample of NFe 90 – 4.5 mm: (a) image of probe before sensing (Al marked with a X), (b) XRT scan (light element in orange), (c) NIR scan (Al coloured in red).

### 3.2.2 XRT detectors

As shown in Figure 9b, XRT scan allows recognising lighter elements (orange / light-green particles) from the rest. In this case, the separation set up as low pass filter where green / blue highlighted particles (Pb, Zn, Cu) were discarded from the rest. The main problems of this strategy were related with the presence of composite materials such as small pieces of electronic waste present in the Al fraction 90 – 4.5 mm or coax-cables which have an inner conductor made of copper surrounded by a tubular insulating layer, surrounded by a tubular conducting shield typically made of Al.

In terms of reliability, the XRT sensor allows detecting between 85 and 90 % of Al (see Figure 7b – XRT). This detector was not only more performant than NIR but also presented fewer deviations.

## 3.3 Al refining

The problems related to Al coming from landfill are related to the proportion of pollutants. Al used to produce foils or packing is in general rather pure. However, once these materials are mixed with organics and inorganics, it is difficult avoiding partial oxidation of Al in a thermal treatment at high temperature. This happens not only by the presence of oxygen in the molten salt but also by the partial reduction of other metal oxides nobler than Al such as Fe, Cu, Si, Ti, Cr present as pollutants.



Comparing the two fractions refined, the purity of the Al recovered in the fines is higher than in the coarse fraction. However, the proportion of metal recovered is 33 % higher in the fraction 200 – 90 mm than in the 90 – 4.5 mm. Apart from soda cans, Al packaging are composites that contains paper and plastics and Al foils have rest of food inside. Besides Al foils are more sensible to oxidation than the rest of Al scrap and consequently the inorganics in the final mass balance are higher. As shown in Figure 10a, both organic and inorganics represent on average the 51 % of the input material.

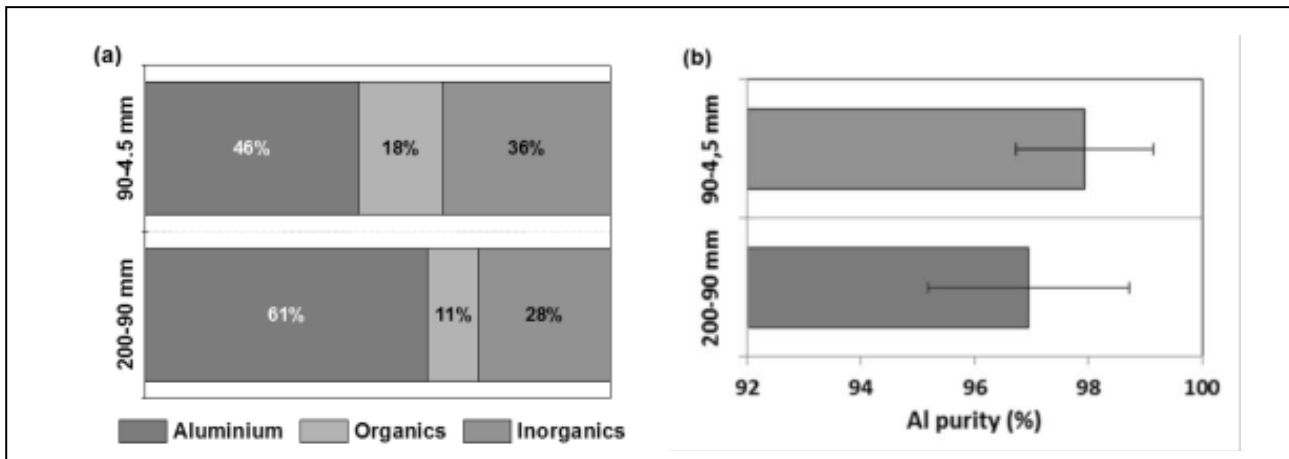


Figure 10: Al refining: (a) proportion of metals vs pollutants; (b) Al-purity obtained.

After smelting, the fraction had completely different results. The fractions  $\geq 90$  mm were rich in construction and demolition materials besides all kind of wires. The problem related with this fraction is, that Al pieces are not completely isolates. Al came together with pieces of iron, copper or brass. Wires are among the most common elements found in the NFe concentrates from this landfill, and from all wires, coax-cables were complicates to separate because the outside mesh is made of Al wires and the centre contains a copper wire. If these wires are identified as Al for the sorting machines, copper will pollute Al during the refining.

The impurities found in the refined Al depend not only on the alloying existing in the starting material, which was the case of the fraction 200 – 90 mm due to the presence of construction and demolition waste, but also of pollutants. The amount pollutants were related with the mechanical processing and the metal sorting technics.

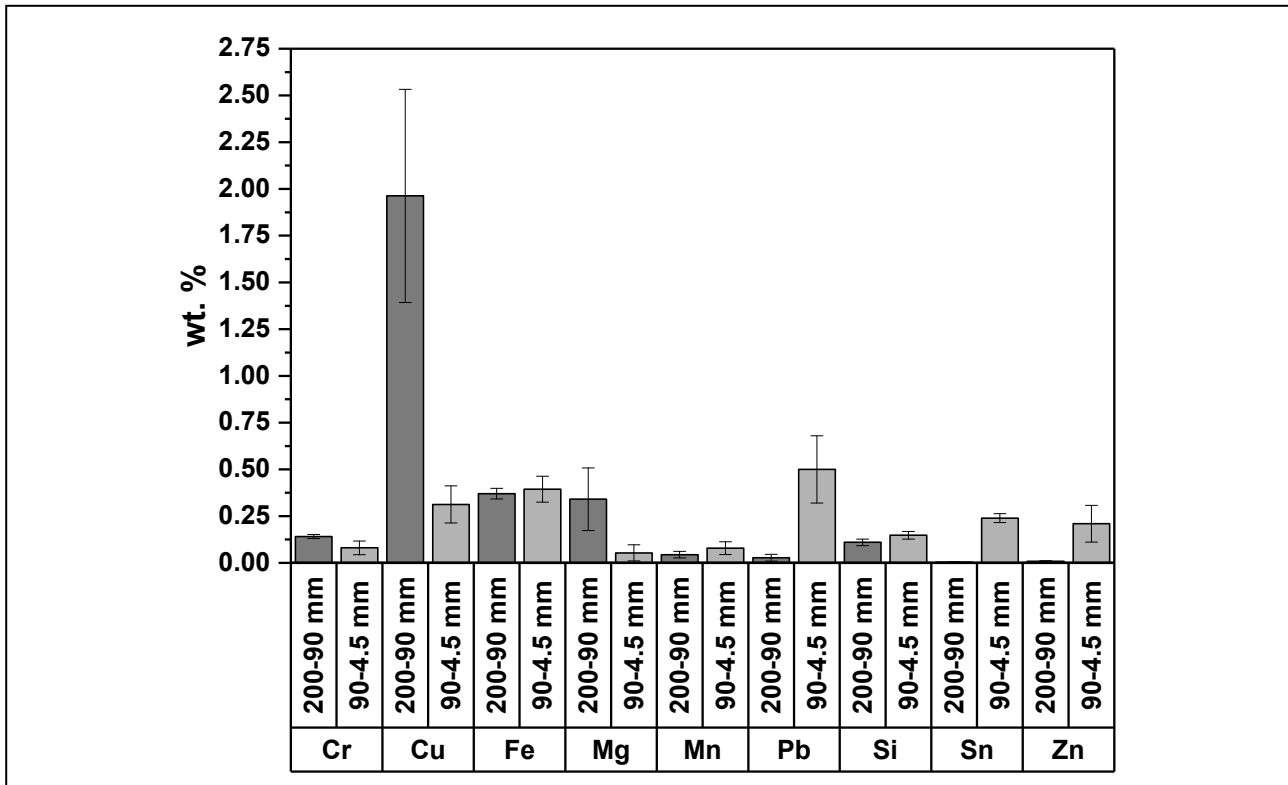


Figure 11: Impurities found in refined Al.

Regarding the mechanical processing, many of these were buried for more than 60 years. The mineral are so bonded that after one hour of ultrasonic cleaning, they still stuck on the surface of the metal. On the other side the type of pollutant found on Al also depends of the separation technique used. In this case XRT sensor was used as low-pass-filter to separate the light elements from the rest and treated as Al. Using XRT as a low pass filter allows for example, contaminated Al scrap with some electronic waste due to the plastic board that contains the electronic components. For this reason trace of Pb, Sn, Zn and Cu are present in the refined Al of the fraction 90 – 4.5 mm (see Figure 11).

Regarding the fraction 200 – 90 mm coax-cables contained Cu also influenced the proportion of this metal in the final product. Finally, elements such as Fe, or Si, existent under the form of oxides inside the inorganics fraction were partially reduced during the smelting.

## 4 Conclusions

Nowadays, Al is the main nonferrous metal recovered from MSW [5]. However, it was not the case of this particular landfill which Al was the second most common NFe metal found behind Cu. The presence of other valuable metals such as Pb, Zn, and Cu are related to the low or null recycling of MSW carried out a few decades ago. This also is why old landfills represent not only an environmental problem but also a potential for metal mining [3].

In the case of the sensors used to detect and separate Al in this study, it was verified that sorting sensors are more effective the cleaner the particles are. The NIR sensor was the most affected when



the metals were found agglomerated and polluted with organics and inorganics on their surface. For this reason, it can be concluded that XRT sensor is more suitable for separating Al from landfill waste than NIR.

For increasing Al quality during the refining, a previous incineration step is required to burn organic matter. This pre-combustion can also favour the separation of those impurities which were deeply attached to the metal after decades of being buried. However, it is necessary to take into account that Al foils, mainly present in the fine fractions (< 90 mm), are sensitive to oxidation, and part of them might be lost during combustion [5].

An Al quality between 97 % and, in some cases, 99 % were achieved, which results quite high taking into consideration the age of the landfill waste, since some of these metals have been landfilled for more than 60 years.

This work seeks to demonstrate that enhanced landfill mining is a necessary step for a sustainable development in our society and metals such as Al can be successfully recycled, even after decades of having been manufactured.

## 5 Acknowledgments

This project has received funding from the European Union's EU Framework Programme for Research and Innovation H2020 under Grant Agreement No 721185.

## 6 References

- [1] Jones P.T., Geysen D., Rossy A., Bienge K., 2010. Enhanced Landfill Mining (ELFM) and Enhanced Waste Management (EWM): Essential components for the transition to Sustainable Materials Management (SMM). Proceedings of the First International Academic Symposium on Enhanced Landfill Mining. 4 – 6 October, 2010. Houthalen-Helchteren, Belgium.
- [2] Van Vossen W.J., Prent O.J., 2011. Feasibility study: Sustainable material and energy recovery from landfills in Europe. Proceedings Sardinia 2011. Thirteen International Waste Management and Landfill Symposium, 247 – 248.
- [3] Hernández Parrodi J.C., Hoellen D., Pomberger R., 2018. Characterization of fine fractions from landfill mining: A review of previous investigations. *Detritus – Multidisciplinary Journal for Waste Resources & Residues*, 42-62. DOI: 10.31025/2611-4135/2018.13663.
- [4] Hernández Parrodi J.C., Hoellen D., Pomberger R., 2018. Potential and main technological challenges for material and energy recovery from fine fractions of landfill mining: A critical review. *Detritus – Multidisciplinary Journal for Waste Resources & Residues*, 19 – 29. DOI: 10.31025/2611-4135/2018.13689.



- [5] Kahle K., Kamuk B., Kallesøe J., Fleck E., Lamers F., Jacobsson L., Sahlén J. Bottom Ash from WTE plants: Metal Recovery and Utilization (No. 2015). ISWA – Working group on energy recovery, Denmark. 2015
- [6] García López C., Ni A., Hernández Parrodi J.C., Kueppers B., Pretz T., 2019. Characterization of landfill mining material after ballistic separation to evaluate material and energy recovery potential. *Detritus – Multidisciplinary Journal for Waste Resources & Residues*.
- [7] Hernández Parrodi J.C., García López C., Raulf K., Pretz T., Kueppers B., Vollprecht D., Pomberger R., 2018. Characterization of Fine Fractions from Landfill Mining - A Case Study of a Landfill Site in Belgium. *Recy & DepoTech 2018*, 569 – 576.
- [8] Bureau d'études greisch, 2002. Centre d'Enfouissement Technique de Mont-Saint-Guibert: Etude des conséquences de l'octroi du permis d'urbanisme du 29.10.01 sur les conditions d'exploitation du permis du 16.12.98.
- [9] D'Or, D., 2013. Modélisation et caractérisation des émissions surfaciques de biogaz sur les C.E.T. en RW: Traitement des données de la campagne de mesures de septembre-octobre 2012 sur le CETeM. Ephesia Consult.
- [10] Gaël, D., Tanguy, R., Nicolas, M., Frédéric, N., 2017. Assessment of multiple geophysical techniques for the characterization of municipal waste deposit sites. *Journal of Applied Geophysics* 145, 74 – 83. 10.1016/j.jappgeo.2017.07.013.
- [11] IGRETEC, 1994. Centre d'Enfouissement Technique de Mont-Saint-Guibert: Etude des incidences sur l'environnement.
- [12] S. Detection, "HI-SCAN 6040i/eX, 6046si und 7555i/si Röntgenprüfgeräte, Technisches Handbuch", Smiths Heimann, 2011.
- [13] Thoraval M., Sieben S., Friedrich B.. Design of a Mini-TRF at IME – Methodology to better understand salt slag interactions with molten aluminium. *World of Metallurgy – ERZMETALL* 67(6): 339 – 345. 2014.
- [14] Mitov, R. (2013): Motion modes of the bed in tube rotary kilns and opportunities for mathematical description of the disperse material behaviour. – *Advances in Natural Science: Theory & Applications*, Vol. 1, Nr. 1: 1-19.